IEEE Access
Multidisciplinary ⋮ Rapid Review ⋮ Open Access Journal

Received October 21, 2021, accepted November 17, 2021, date of publication November 25, 2021,
date of current version December 9, 2021.

Digital Object Identifier 10.1109/ACCESS.2021.3130637

Compound Fault Diagnosis of Aero-Engine Rolling Element Bearing Based on CCA Blind Extraction

WEI-TAO ZHANG[1], XIAO-FAN JI[1], JU HUANG[2], AND SHUN-TIAN LOU[1], (Member, IEEE)
[1]School of Electronic Engineering, Xidian University, Xi'an 710071, China
[2]Research Institute of Guiyang Engine Design of Aero Engine Corporation of China, Guiyang 550081, China

Corresponding author: Wei-Tao Zhang (zhwt-work@foxmail.com)

This work was supported by the National Natural Science Foundation of China under Grant 62071350.

ABSTRACT Fault diagnosis of aero-engine spindle bearing is a critical technique of engine prognostics and health management. As is known that the diagnosis of compound fault of aero-engine spindle bearing is very difficult and easily affected by other vibration interference signals. We present a canonical correlation analysis (CCA) criterion based method for blind extraction of specific fault signal from multi-channel observations, which is applicable to compound fault diagnosis of aero-engine spindle bearing. The proposed method uses the different fault characteristic frequency of rolling element bearing to estimate the delay parameter in CCA criterion. The conjugate gradient method is adopted to optimize the CCA criterion, which not only speed up the convergence of the optimization algorithm, but also improves the reliability of the resulted algorithm. Both the simulated data and the experimental data are used to verify the effectiveness of the algorithm in compound fault diagnosis.

INDEX TERMS Blind signal extraction, rolling bearing, fault diagnosis.

I. INTRODUCTION

Rolling element bearing is one of the most prevalent components in rotating machines, and their failure is one of the most frequent reasons for machine breakdown. Because the aero-engine spindle bearing works in the harsh working conditions of high temperature, high speed and heavy load for a long time, the weak faults in the early stage will quickly become serious faults, which eventually cause terrible disasters in various applications. Robust health monitoring tools are needed to guarantee the healthy state of rolling element bearing during the operation. However, there are several challenges to extract the features related to the faulty rolling element bearing, e.g. the removal of back-ground noise effect and the suppression of other interference components. A most challenging task is to deal with the compound fault. Specially, in the early stage of fault where the defect is quite small and can be easily buried by other vibration interferences, Compound fault can be rarely detected and identified from the observations.

In recent years, many experiments and studies have been performed in the literature for rolling bearing compound fault diagnosis [1]–[4], including method based on temperature signal or vibration signal. The method based on temperature signal [5] diagnoses the bearing fault by monitoring the change of temperature. However, the temperature is a slowly varying quantity, which almost keeps constant for small defect bearing. So it is not suitable for the fault diagnosis of aero-engine spindle bearing in the early stage. In addition, it is difficult to determine the specific location of the defect through the change of temperature, so it is not yet suitable for the compound fault diagnosis. Methods based on vibration monitoring can be divided into two categories, the signal processing-based fault detection methods and the machine learning-based fault detection methods. The former include traditional spectrum analysis method, spectral kurtosis method, blind signal separation method, blind signal extraction method and nonlinear dynamics-based fault detection method. The traditional spectrum analysis method can directly read the fault characteristic frequency from the envelope spectrum to determine the fault categories. However, the defect in the early stage is so small that its frequency component in the envelope spectrum is prone to be buried by other vibration interferences. Therefore, the traditional envelope spectrum analysis method often fails for the detection of defect in early stage. The maximum correlation kurtosis deconvolution (MCKD) method [6]–[10] considers that the vibration signal is the result of the convolution of the periodic

The associate editor coordinating the review of this manuscript and approving it for publication was Amir Masoud Rahmani.

impact signal caused by the fault and the resonance response of other mechanical parts. Therefore, the deconvolution signal of the specified period can be extracted by setting the corresponding fault shift period and regarding the signal with the maximum correlation kurtosis as the interference component. However, there are many input parameters of MCKD (such as filter length and shift bits), and the algorithm is very sensitive to the parameter values, which means only when all parameters are reasonably selected, can MCKD play its advantages in extracting periodic fault impulse signal, which greatly limits its practical application. Some improved methods based on traditional methods are also proposed [11]–[15]. Artificial neural network method has also been applied in the field of bearing fault diagnosis, including shallow machine learning model and deep machine learning model. Shallow machine learning model, such as artificial neural network and support vector machine [16]–[18], has to extract a series of features (such as variance, energy entropy, root mean square, etc.) manually and use the extracted features as the input of the model. However, this kind of method depends heavily on the selection of features, and it is very difficult to select features with obvious differentiation under complex conditions. Deep learning methods [19]–[25] such as generative countermeasure network and convolutional neural network (CNN) avoid feature extraction based on artificial experience. The network automatically finds features in massive data with better generalization. However, the existing CNN models usually achieve the prediction for fault classification purpose only, it cannot extract the fault component from the observations for further analysis. Moreover, when there are strong interference signals, the classification performance degraded sharply. Besides the deep learning method needs a lot of training data, but it is almost unrealistic to obtain massive data under complex time-varying conditions because the spindle bearing speed and load change rapidly and widely.

Note that most of the above methods deal with the observed signals directly. However, they usually fail because the collected vibration signals of the aero-engine spindle bearing are actually mixed signals of different vibration sources. The first reason is that the faults of the spindle bearing of the long-term operation are usually compound faults, for example, the entering of foreign body into the bearing may cause scratches on both the inner race and outer race at the same time. Compound faults will lead to multiple components in observations, which contribute more or less to the observations with unknown impact factors; another reason is that due to the complicated internal structure of the aero-engine and the limitation of high temperature environment, the sensors used for bearing condition monitoring cannot be equipped on the bearing seat or other parts nearby in actual working conditions. The vibration signal collected by each sensor is usually a comprehensive reflection of the vibration of the bearing and other components, such as oil pump. In addition, the bearing rotor system with local fault may have typical nonlinear resonance such as superharmonic resonance and subharmonic resonance [26]. Therefore, it is often unreliable to use the sensor observed signals for fault diagnosis directly.

Considering the particularity of compound fault analysis of aero-engine spindle bearing, the restoration of the specific fault signal from multiple observations can be solved by separating the fault signal and other interference signals from the collected vibration signals. There are two kinds of methods to accomplish this task, the first one is the blind signal separation method (BSS), which can separate different signals simultaneously [27], the other is the blind signal extraction method (BSE), which extract different source signals successively by using deflation procedure. Compared with blind separation method, blind extraction method has some advantages: the first one is that it can save the computational cost when we are only interested in a specific source signal; the second one is that we can still restored the source signal of interest via BSE when simultaneous separation of all sources is difficult to accomplish in some ill-conditioned scenario. In general, BSE is more flexible than BSS. This paper focuses on the extraction of the specific bearing fault vibration signal, so BSE method is more suitable for aero-engine bearing fault diagnosis.

Typical BSE methods include FastICA [28] and other methods based on higher-order statistics. However, the extraction order of source signals for these methods has not been well studied, and it is unknown in real applications. In addition, how to take advantage of the prior information of sources to extract the signal of interest is still unresolved. Canonical correlation analysis (CCA) [29] has also been proved to be an effective BSE method. Although some online realizations of this approach have been proposed using linear prediction, the resulting algorithms are gradient search method, suffering from slow convergence rate. In fact, gradient learning algorithm with stable convergence is still expected, because the existing steepest descent learning algorithm often leads to failed extraction. To overcome these drawbacks, we propose to consider the conjugate gradient optimization for the CCA criterion [30], [31], which is expected to greatly improve the convergence speed and stability of the learning algorithm. The relationship between the delay parameter of CCA criterion and the characteristic frequency of bearing fault is discussed. Finally the proposed method is applied to the diagnosis of aero-engine rolling element bearing. A large number of simulation and experimental results verify the effectiveness of the proposed method. It should be pointed out that the proposed method is readily to be extended to the real-time monitoring of aero-engine spindle bearing, which can detect weak faults as early as possible. This enables to transform the engine regular maintenance into predictive maintenance, so as to reduce the cost of maintenance.

II. CCA CRITERION FOR BLIND SIGNAL EXTRACTION

If multiple sensors are used to capture the vibrations of aero-engine spindle bearing, the multi-channel observation signals can be expressed as a linear mixture of multiple independent

vibration sources. The instantaneous mixing model commonly reads

$$\mathbf{x}(t) = \mathrm{A}\mathbf{s}(t) \tag{1}$$

where $\mathbf{x}(t) = [\mathbf{x}_1(t), \ldots, \mathbf{x}_M(t)]^T$ is the vector of mixed signals, $\mathbf{s}(t) = [\mathbf{s}_1(t), \ldots, \mathbf{s}_N(t)]^T$ is the vector of unknown sources, A is a $M \times N$ ($M \geq N$) unknown mixing matrix, which contains the path attenuation coefficients from different vibration sources to multiple sensors. The task now is to design an extraction vector to extract signal from multichannel observations.

$$y(t) = \mathbf{w}^T\mathbf{x}(t) \tag{2}$$

The basic idea behind the CCA approach is that the sum of any uncorrelated signals has an autocorrelation whose value is less than or equal to the maximum value of individual signals. Thus, the CCA approach maximize the normalized time delayed autocorrelation of the extracted signal $\mathbf{y}(t)$ with respect to the extraction vector $\mathbf{w}$

$$\arg\max_{\mathbf{w}} \bar{J}(\mathbf{w}) = \frac{E[y(t)y(t-\tau)]}{E[y^2(t)]} = \frac{\mathbf{w}^T\mathbf{R}_{\mathbf{x}}^{\tau}\mathbf{w}}{\mathbf{w}^T\mathbf{R}_{\mathbf{x}}^{0}\mathbf{w}} \tag{3}$$

where $\mathbf{R}_{\mathbf{x}}^{\tau}$ is the time delayed correlation matrix of mixed signal and $\mathbf{R}_{\mathbf{x}}^{0}$ is the covariance matrix of the mixed signals. It can be seen that the optimal solution is typically obtained by taking $\mathbf{w}$ to be the generalized eigenvector of matrix pencil $(\mathbf{R}_{\mathbf{x}}^{\tau}, \mathbf{R}_{\mathbf{x}}^{0})$ associated with the maximum generalized eigenvalue. Clearly, the existence of the solution for sequentially extracting all the sources via CCA approach can be guaranteed if the generalized eigenvalues are different from each other. It is also interesting to note that the uniqueness condition of CCA approach for source extraction is that the source signals have different normalized spectra, which enlightens us that we can extract the signal of interest by optimizing CCA criterion and selecting the appropriate time delay τ.

Several online algorithms have been proposed based on the CCA criterion. However, these algorithms use a gradient descent technique and hence suffer from slow convergence rate. In addition, the convergence of the gradient learning algorithms is very sensitive to the mixing process, which leads to a lower successful rate in real applications. In the next section, we present a conjugate gradient algorithm to improve the convergence of the CCA-based online extraction algorithms.

III. BLIND CCA EXTRACTION ALGORITHM BASED ON CONJUGATE GRADIENT

In this section, we firstly introduce the conjugate direction in the optimization problem, and then a conjugate gradient algorithm is derived to extract one signal source through optimizing the CCA criterion equation (3). Finally, we summarize the proposed optimization algorithm, and discuss how to determine the time delay τ to apply the algorithm to the compound fault diagnosis of rolling bearing.

A. CONJUGATE DIRECTION

Given a symmetric positive definite matrix $\mathbf{Q}$, two vectors $\mathbf{d}_1$ and $\mathbf{d}_2$ are said to be $\mathbf{Q}$-orthogonal, or conjugate with respect to $\mathbf{Q}$, if $\mathbf{d}_1^T\mathbf{Q}\mathbf{d}_2 = 0$. A finite set of vectors $\{\mathbf{d}_1, \ldots, \mathbf{d}_n\}$ is said to be $\mathbf{Q}$-orthogonal set if $\{\mathbf{d}_1, \ldots, \mathbf{d}_n\}$ for all $1 \leq i \neq j \leq n$.

Given a quadratic convex function

$$f(\mathbf{x}) = \frac{1}{2}\mathbf{x}^T\mathbf{Q}\mathbf{x} + \mathbf{k}^T\mathbf{x} + c \tag{4}$$

where $\mathbf{Q}$ is symmetric positive definite. Let us denote ψ_k as the subspace spanned by a set of $\mathbf{Q}$-orthogonal vectors $\mathbf{d}_1, \cdots, \mathbf{d}_k$, or for short

$$\psi_k = \left\{ \mathbf{x} | \, \mathbf{x} = \sum\nolimits_{i=1}^{k} \mu_i \mathbf{d}_i, \mu_i \in (-\infty, +\infty) \right\} \tag{5}$$

The sequence $\mathbf{x}_2, \ldots, \mathbf{x}_{k+1}$ converges to the unique solution $\mathbf{x}^*$ of $\mathbf{Q}\mathbf{x} + \mathbf{k} = 0$ after n steps. In other words, $\mathbf{x}^*$ is the minimizer of equation (4).

This theorem implies that for quadratic convex functions, the conjugate gradient algorithm converges to the unique global minimum after finite steps, as long as the update is conducted along the non-interfering searching directions. This inspires us to find the conjugate direction of problem equation (3) and derive the conjugate gradient algorithm to improve the convergence of the algorithm.

B. DERIVATION OF BLIND SIGNAL EXTRACTION ALGORITHM

Although theorem is applied to the optimization for quadratic convex functions, we can always generalize the conjugate gradient algorithm to devise a numerical routine to minimize an arbitrary function. Here the Hessian of the cost function equation (3) plays the role of Q. Note that the optimization of equation (3) is the problem of maximizing the CCA cost function. Let $J(\mathbf{w}) = -\bar{J}(\mathbf{w})$, so that the maximization problem is transformed into minimization problem. The conjugate gradient algorithm selects the successive directions vectors as a conjugate version of the successive gradients, then the minimum point can be reached after finite steps.

Since the conjugate gradient algorithm is based on gradient, we write the gradient and Hessian matrix of cost function $J(\mathbf{w})$ with respect to $\mathbf{w}$ as $\mathbf{g} \triangleq \nabla_{\mathbf{w}} J(\mathbf{w})$ and $\mathbf{H} \triangleq \nabla_{\mathbf{w}}^2 J(\mathbf{w})$, where ∇ represents gradient operator. Note that the initial value of $\mathbf{w}$ can be randomly chosen, the empirical choice is $\mathbf{w}_1 = [1, \cdots, 1]^T$, whereas the initial search direction $\mathbf{d}_1$ should be the steepest descent direction

$$\mathbf{d}_1 = -\nabla_{\mathbf{w}_1} J(\mathbf{w}_1) = -\mathbf{g}_1 \tag{6}$$

At step t one evaluates the steepest descent direction $-\mathbf{g}_t$. Based on this direction, the current conjugate direction can be obtained by adding a scaled version of previous conjugate direction vector with the scale factor ρ_{t-1}

$$\mathbf{d}_t = -\mathbf{g}_t + \rho_{t-1}\mathbf{d}_{t-1} \tag{7}$$

where the factor ρ_{t-1} is chosen to provide $\mathbf{Q}$-conjugacy for the vector $\mathbf{d}_t$ with respect to the previous direction vectors

$\mathbf{d}_{t-1}, \mathbf{d}_{t-2}, \ldots, \mathbf{d}_0$. In order to ensure that the search direction $\mathbf{d}_t$ and $\mathbf{d}_{t-1}$ are conjugate with the Hessian matrix, the following equation must be satisfied

$$\mathbf{d}_t^T \mathbf{H}_{t-1} \mathbf{d}_{t-1} = 0, \tag{8}$$

The substitution of equation (7) into equation (8) leads to

$$\rho_{t-1} = \frac{\mathbf{g}_t^T \mathbf{H}_{t-1} \mathbf{d}_{t-1}}{\mathbf{d}_{t-1}^T \mathbf{H}_{t-1} \mathbf{d}_{t-1}} \tag{9}$$

Although equation (9) only ensures that the search directions of the two adjacent iterations are **Q**-orthogonal vectors, it is proved that as long as the initial search direction is the steepest descent direction, the set of search directions $\mathbf{d}_1, \ldots, \mathbf{d}_t$ $(t > 1)$ generated by equation (7) are non-zero **Q**-orthogonal vectors.

For tth iteration, the extraction vector $\mathbf{w}$ can be updated by

$$\mathbf{w}_{t+1} = \mathbf{w}_t + \eta_t \mathbf{d}_t \tag{10}$$

where η_t is the step size. In order to speed up the converge of the resulting algorithm, the step size η_t can be also viewed as a variable that can be estimated via the following optimization

$$J(\mathbf{w}_{t+1}) = \min_{\eta} J(\mathbf{w}_t + \eta \mathbf{d}_t) \tag{11}$$

Let $\varphi(\eta) = J(\mathbf{w}_t + \eta \mathbf{d}_t)$, the optimal iteration step size should satisfy $\frac{d\varphi(\eta)}{d\eta} = 0$. The solution is straightforward

$$\mathbf{d}_t^T \nabla_{\mathbf{w}_{t+1}} J(\mathbf{w}_{t+1}) = 0 \tag{12}$$

Note that the gradient and Hessian of $J(\mathbf{w})$ with respect to $\mathbf{w}$ plays an important role computing conjugate direction, it can be readily shown that

$$\mathbf{g} = \frac{(\mathbf{w}^T \mathbf{R}_{\mathbf{x}}^{\tau} \mathbf{w}) \mathbf{R}_{\mathbf{x}}^0 - (\mathbf{w}^T \mathbf{R}_{\mathbf{x}}^0 \mathbf{w}) \mathbf{R}_{\mathbf{x}}^{\tau}}{(\mathbf{w}^T \mathbf{R}_{\mathbf{x}}^0 \mathbf{w})^2} \mathbf{w}, \tag{13}$$

Let $a = \mathbf{w}^T \mathbf{R}_{\mathbf{x}}^0 \mathbf{w}$, $b = \mathbf{w}^T \mathbf{R}_{\mathbf{x}}^{\tau} \mathbf{w}$, $\mathbf{g}$ can be computed by

$$\mathbf{g} = \frac{b \mathbf{R}_{\mathbf{x}}^0 - a \mathbf{R}_{\mathbf{x}}^{\tau}}{a^2} \mathbf{w} \tag{14}$$

The Hessian matrix is given by

$$\mathbf{H} = \frac{b \mathbf{R}_{\mathbf{x}}^0 - a \mathbf{R}_{\mathbf{x}}^{\tau}}{a^2} \tag{15}$$

To achieve an online realization of the algorithm, matrices $\mathbf{R}_{\mathbf{x}}^{\tau}$ and $\mathbf{R}_{\mathbf{x}}^0$ should be replaced by their sample estimate and recursively computed as

$$\begin{aligned} \mathbf{R}_{\mathbf{x}}^{\tau}(t) &= \beta \mathbf{R}_{\mathbf{x}}^{\tau}(t-1) + \mathbf{x}(t)\mathbf{x}^T(t-\tau) \\ \mathbf{R}_{\mathbf{x}}^0(t) &= \beta \mathbf{R}_{\mathbf{x}}^0(t-1) + \mathbf{x}(t)\mathbf{x}^T(t) \end{aligned} \tag{16}$$

where $0 < \beta < 1$ is the forgetting factor. In addition, $\mathbf{R}_{\mathbf{x}}^{\tau}(t)$ is usually replaced by its symmetrical version in practical implementations. The coefficient a and b can be recursively computed as

$$\begin{aligned} a_t &= \beta a_{t-1} + y^2(t) \\ b_t &= \beta b_{t-1} + y(t)y(t-\tau) \end{aligned} \tag{17}$$

The substitution of equation (14) and (15) into equation (12) leads to

$$\mathbf{d}_t^T \mathbf{H}_{t+1}(\mathbf{w}_t + \eta_t \mathbf{d}_t) = 0 \tag{18}$$

Then the optimal step size is given by

$$\eta_t^* = -\frac{\mathbf{d}_t^T \mathbf{H}_{t+1} \mathbf{w}_t}{\mathbf{d}_t^T \mathbf{H}_{t+1} \mathbf{d}_t} \tag{19}$$

According to the above derivation, the substitution of equation (16) and (17) into equation (14) and (15) leads to the adaptive conjugate gradient algorithm. However, it can be seen that

$$\mathbf{H}_{t+1} = \frac{[\mathbf{w}_{t+1}^T \mathbf{R}_{\mathbf{x}}^{\tau}(t) \mathbf{w}_{t+1}] \mathbf{R}_{\mathbf{x}}^0(t) - [\mathbf{w}_{t+1}^T \mathbf{R}_{\mathbf{x}}^0(t) \mathbf{w}_{t+1}] \mathbf{R}_{\mathbf{x}}^{\tau}(t)}{[\mathbf{w}_{t+1}^T \mathbf{R}_{\mathbf{x}}^0(t) \mathbf{w}_{t+1}]^2} \tag{20}$$

Take equation (10) into consideration, the closed form solution for step size η_t cannot be obtained by equation (19) because $\mathbf{H}_{t+1}$ also depends on step size η_t. To overcome this problem and simplify the optimization with respect to step size, let us recall that a fixed small step size for gradient learning still performs well. So we propose to firstly update the blind extraction vector $\mathbf{w}$ according to equation (10) with a small step size, so as to obtain $\hat{\mathbf{w}}_{t+1}$ temporarily, and then we substitute $\hat{\mathbf{w}}_{t+1}$ into equation (20) to get $\mathbf{H}_{t+1}$, finally substituting $\mathbf{H}_{t+1}$ into equation (19) leads to the optimal step size. Without losing generality, we simply use $\eta_t = 0$, then we have $\hat{\mathbf{w}}_{t+1} = \mathbf{w}_t$ and $\mathbf{H}_{t+1} = \mathbf{H}_t$. This can not only ensure the convergence of the algorithm, but also avoid the tedious iterative operation between equation (10), (20) and (19).

TABLE 1. The CCA blind signal extraction algorithm based on conjugate gradient.

Initialization:
a) initialize time delay τ, extraction vector $\mathbf{w}_1$;
b) initialize search direction $\mathbf{d}_1 = -\mathbf{g}_1$;
c) initialize $\mathbf{R}_{\mathbf{x}}^0(0)$, $\mathbf{R}_{\mathbf{x}}^{\tau}(0)$,$a_0$ and b_0;
For $t = 1, 2, \ldots$ do:
a) compute output signal $\mathbf{y}(t)$ according to equation (2);
b) compute gradient and Hessian matrix according to equation (14) - (17). If the current gradient is small enough, the iteration is stopped, otherwise the iteration is continued;
c) compute extraction vector w according to equation (19) and (10);
d) compute search direction of the next iteration according to equation (7) and (9).

C. APPLICATION OF ALGORITHM IN BEARING FAULT DIAGNOSIS

Combining the results obtained so far, a CCA adaptive blind signal extraction algorithm based on conjugate gradient can be summarized in Table (1). Here we need to pay special attention to the following three points: (1) In order to ensure that the generated search direction is conjugate with respect to the Hessian matrix, the initial search direction must be the steepest descent direction; (2) Different from the quadratic convex function, the Hessian matrix of arbitrary cost function

cannot be guaranteed to be always positive definite, so in general, the conjugate gradient algorithm cannot achieve convergence in a few finite steps; (3) the conjugate gradient algorithm can be implemented by either continuous iteration or discontinuous one. We recommend executing groups of M search steps. After M iteration steps, the algorithm resets with its current $\mathbf{w}$ as a new ''origin'', from which we start another M search steps. This method can eliminate the accumulation error of continuous conjugate direction iteration.

In addition, the amplitudes of the shocks are subjected to modulations by the rotations of the inner race (inner race fault), the outer race (outer race fault) or the cage (element fault). Among these types of faults, the inner race fault and outer race fault are more common, and They are usually compound faults in most scenarios. For example, the entering of small rigid foreign body into the bearing will cause defects on both the inner and outer race. Due to the particularity of the working environment of aero-engine spindle bearing, the sensors cannot be directly arranged near the bearing, but can be only arranged on the non-rotating parts or the gearbox. Thus the vibration signals collected by the sensors are comprehensive reflection of the vibration caused by the fault point of the bearing and other vibration sources. In order to extract bearing fault signal from observed vibration signal, some prior knowledge involving bearing fault signals have to be exploited. The high-speed rotation of the shaft often leads to the bearing fault signal with cyclostationarity, which can be characterized by the cycle frequency of the fault signal, and different types of faults have different cycle frequencies, also known as the fault characteristic frequency. Therefore, the fault characteristic frequency can be used to extract the specific fault signal. The inner and outer fault characteristic frequencies read

$$f_i = \frac{n}{2*60}(1 + \frac{d}{D_m}\cos\alpha)z, \tag{21}$$

$$f_o = \frac{n}{2*60}(1 - \frac{d}{D_m}\cos\alpha)z, \tag{22}$$

where f_i is the inner race fault characteristic frequency, f_o is the outer race fault characteristic frequency, n is the shaft speed, α is the contact angle, D_m is the pitch diameter, z is the number of rolling elements, d is the roller diameter.

For the proposed algorithm, it is necessary to ensure that the time delayed autocorrelation of the target fault signal has the maximum value. As for the cyclostationary signal, the fault signal has the maximum autocorrelation at the time delay associated with the cyclic frequency. Therefore, the time delay τ in the CCA criterion should be the one corresponding to the cyclic frequency of the target fault signal. Take the extraction of the inner race fault signal as an example, the time delay can be computed by

$$\tau_i = 1/f_i, \tag{23}$$

By choosing corresponding time delay τ, one can extract the fault signal of interest using the algorithm in Table (1).

IV. SIMULATION AND EXPERIMENTAL RESULTS

In this section, some simulation and experimental results are presented to demonstrate the performance of the proposed CCA adaptive blind signal extraction algorithm based on conjugate gradient in compound fault diagnosis of aero-engine spindle bearing. In the simulation, we test our algorithm for the well-known bearing data from Western Reserve University [32], and the mixing matrix is randomly generated. In the experiment, we test our algorithm for the real-world data measured from aero-engine rolling bearing element bearing with compound faults. The proposed algorithm is used for the diagnosis of the compound faults.

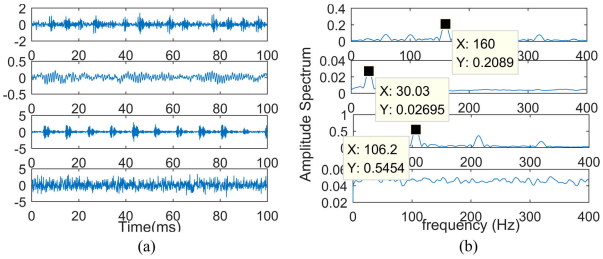

FIGURE 1. Source signals. (a) time signals; (b) envelope spectra.

A. SIMULATION RESULT

The source signals are the bearing vibration signal from Case Western Reserve University (CWRU) Bearing Data Center. It can be seen that the data sets are grouped into three categories- inner race fault, outer race fault and normal bearing vibration signals. In addition, in order to simulate the noise environment, a Gaussian white noise signal is randomly generated as the background noise source. The source signals are shown in Fig. 1.

It can be seen from Fig. 1 (b) that the inner race fault characteristic frequency of the source signal is 159.7Hz, and the outer race fault characteristic frequency is 106.2Hz, and the high-order harmonic can be seen. The existence of high-order harmonic is due to the misalignment in the actual bearing installation process. The more serious the misalignment, the more obvious the high-order harmonic that exists in the vibration signal. It can be seen from Fig. 1 that the envelope spectrum of the second source signal only contains an obvious frequency component of 30.3Hz, which means it is the vibration signal of the healthy bearing. The elements of mixing matrix are randomly generated from a standard normal distribution, so the mixed signals are comprehensive reflection of the inner ring and outer ring fault components. The envelope spectrum of the observed signal from channel 1 is shown in Fig. 2, where the vertical red line and magenta line represent the outer race fault frequency (159.8Hz) and the inner race fault frequency (109.7Hz) computed by equation (21) and (22) respectively. One can easily find the inner race fault frequency of 159.7Hz. However, the outer race fault component of 106.2Hz is buried by noises and other interferences. Therefore, it is necessary to extract latent source sig-

nals from the observations for further analysis. CCA adaptive blind signal extraction algorithm based on conjugate gradient is used to extract inner race fault signal and outer race fault respectively.

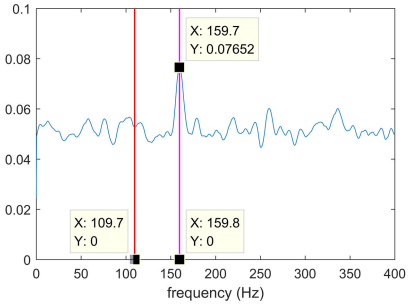

FIGURE 2. Envelope spectrum of observed signal (channel 1).

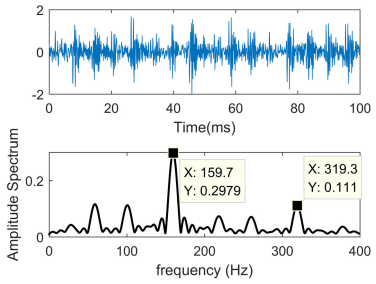

FIGURE 3. Extracted inner race fault signal.

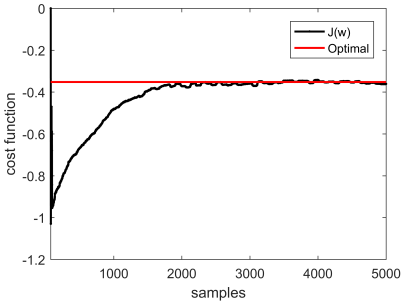

FIGURE 4. Convergence curve of the cost function for inner race fault signal extraction.

We set $\tau_i = 6.26ms$ to extract the inner race fault signal. Fig. 3 shows the inner race fault signal extracted by the proposed algorithm. We see that the proposed algorithm can successfully extract the inner race fault component with frequency of 159.7Hz, which verifies the effectiveness of the proposed algorithm. Fig. 4 shows the learning curve of the cost function. The red line represents the cost function value corresponding to the optimal solution, and the black line is the cost function change curve in the actual iteration. We find that the cost function converges rapidly to the optimal value in 2000 iterations.

We set $\tau_o = 9.42ms$ to extract the outer race fault signal. Fig. 5 shows the outer race fault signal extracted by the

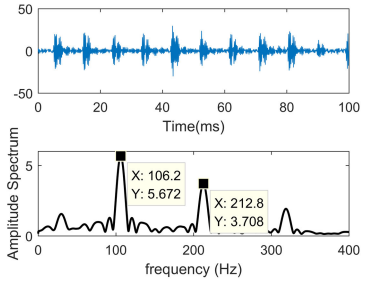

FIGURE 5. Extracted outer race fault signal.

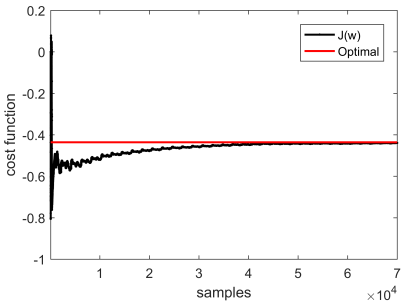

FIGURE 6. Convergence curve of the cost function for outer race fault signal extraction.

proposed algorithm. We see that the proposed algorithm can successfully extract the inner race fault signal with frequency of 106.2Hz. In addition, we can also see high-order harmonic in the envelope spectrum, which is an obvious outer race fault feature. Fig. 6 shows the learning curve of the cost function. We find that the cost function converges rapidly to the optimal value, which verifies the effectiveness of the proposed algorithm.

B. EXPERIMENTAL RESULT

In the experiment, we designed the experimental to detect the vibration signal from the aero-engine rolling element bearing with compound fault, using a three point contact ball bearing with two-piece inner race. The dimension parameters of the bearing are shown in Table 2. The front fulcrum thrust bearing supporting the high-pressure compressor in the aero-engine. It mainly sustains the axial and radial loads, works in the harsh working conditions.

TABLE 2. Bearing size parameters.

Inside Diameter (mm)	Outside Diameter (mm)	Thickness (mm)	Number of balls	Ball Diameter (mm)	Pitch Diameter (mm)	Contact angle (degree)
144.6	188.0	33	17	24.6	166	37

The experimental bearing is a waste bearing removed from an aero-engine during the routine maintenance. Slight pitting corrosion fault is found on both the inner and outer race, which is a typical compound fault bearing. The dataset used in this study was collected using 8 sensors at a sampling rate

of 20kHz. It should be noted that the shaft speed is 1000rpm, and the rotation frequency is 16.67Hz. In addition, the fault characteristic frequency of inner race is 158.43Hz and that of outer race is 124.9Hz according to equation (21) and (22). Three sensors are equipped on the bearing seat and five sensors are equipped on the gearbox of the testing machine. The specific configuration of the accelerometers is shown in Fig. 7.

Since the accelerometers equipped on gearbox are far from shaft and bearing, the bearing fault component and other interference component are uniformly distributed in observed signal. We select the signal obtained by the sensor AC2 for envelope spectrum analysis, and the results are shown in Fig. 8. The vertical lines with different colors in Fig. 8 represent the different theoretically characteristic frequency, among them the blue line represents the rotation frequency (16.67Hz), the red line represents the outer race fault characteristic frequency (124.9Hz), and the magenta line represents the inner race fault characteristic frequency (158.43Hz). It can be seen from the envelope spectrum that the signal is very weak, but the rotation frequency (17.09Hz), the outer race fault characteristic frequency (125.7Hz) and the inner race fault characteristic frequency (159.9Hz) can be clearly seen. It can be seen that in the actual working conditions, the vibration signal observed by each sensor is often a comprehensive reflection of multiple vibration sources, and the transmission path and attenuation are also unknown. It is unreliable to use the collected signals for fault analysis directly. Using blind signal extraction technology to extract the fault signals from the observed signals can effectively suppress the interference and provide more reliable information for subsequent fault analysis and classification identification. To evaluate the performance of the blind extraction algorithms, we use the signal to interference ratio (SIR) as our performance measure, which is defined as

$$\mathrm{SIR} = \rho_s / \rho_i \tag{24}$$

where ρ_s is the amplitude of the target fault characteristic frequency, ρ_i is the amplitude of the maximum interference frequency after removing the target fault characteristic frequency. For example, when extracting the inner race fault signal, the maximum interference is the outer race fault signal because they are the two main vibration sources in this experiment. Similarly, when extracting the outer ring fault, the largest interference is the inner race fault signal. Clearly if SIR is very large, then the corresponding algorithm results in perfect extraction. Fig. 9 and Fig. 10 shows the extracted inner race fault signal and outer race fault signal by the proposed algorithm respectively.

We set $\tau_i = 6.25ms$ to extract the inner race fault signal. Fig. 9 shows the inner race fault signal extracted by the proposed algorithm. We see that the proposed algorithm can successfully extract the inner race fault signal (159.9Hz), and the signal-to-interference ratio is SIR = 1.97. It is also obvious from Fig. 9 (a) that other interference components are also obviously suppressed. Fig. 9 (b) shows the learning

FIGURE 7. Sensor configuration of the experiment system. (a) arrangement of sensors on the gearbox; (b) arrangement of sensors on the bearing seat.

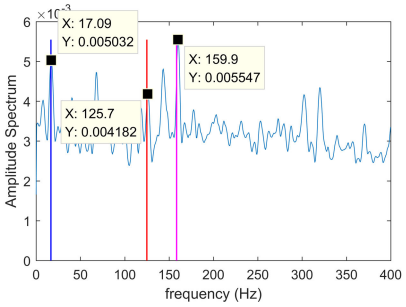

FIGURE 8. Envelope spectrum of the acquisition signal(channel 2).

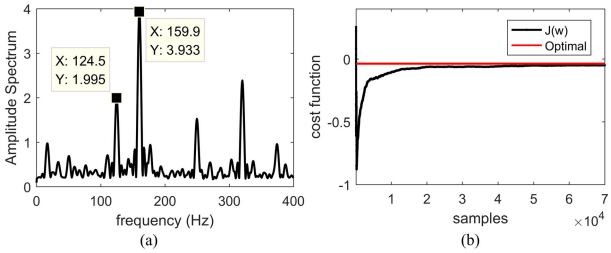

FIGURE 9. Extracted inner race fault signal. (a) envelope spectrum of the extracted signal; (b) convergence curve of the cost function.

curve of the cost function. The red line represents the cost function value corresponding to the optimal solution, and the black line is the cost function change curve in the actual iterations. We find that the cost function converges rapidly to the optimal value and the extracted vector converges to the optimal solution.

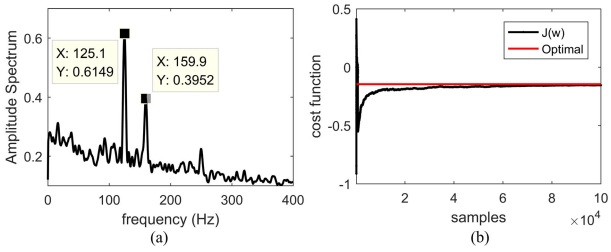

FIGURE 10. Extracted outer race fault signal. (a) envelope spectrum of the extracted signal; (b) convergence curve of the cost function.

We set $\tau_o = 7.96ms$ to extract the outer race fault signal. Fig. 10 shows the outer race fault signal extracted by the proposed algorithm. We see that the proposed algorithm can successfully extract the outer race fault signal (125.1Hz), and the signal-to-interference ratio is SIR = 1.56. It is also obvious from Fig. 10 (a) that other interference components are also obviously suppressed. We find that the cost function converges rapidly to its theoretical value from Fig. 10 (b). Comparing the results of Fig. 9 and Fig. 10, it can be seen that the conjugate gradient CCA blind extraction algorithm has better extraction effect on the inner race fault signal, which is mainly because the inner race defect of the fault bearing is more obvious than the outer race, and the amplitude of the inner race is larger than that of the outer ring. The above results validated our theoretical analysis.

V. CONCLUSION

In this paper, we present a CCA blind extraction method for compound fault diagnosis of aero-engine spindle bearing based on multi-channel signal processing. Although some online realizations of this approach have been proposed using linear prediction, the resulting algorithms are gradient search method, suffering from slow convergence rate. In addition, the convergence of gradient learning algorithms is unresolved. This often leads to failed extraction. To overcome these drawbacks, we use conjugate gradient method to optimize the CCA cost function. In order to ensure that the update direction of the extracted vector in each iteration satisfy the conjugate condition, the conjugate gradient algorithm selects the successive directions vectors as a conjugate version of the successive gradients, then the minimum point can be reached after finite steps. Finally, the CCA blind signal extraction algorithm based on conjugate gradient method is applied to the diagnosis of aero-engine rolling element bearing. The estimation of CCA delay parameter is discussed, and the inherent relationship between fault characteristic frequency and delay parameter is pointed out. Both the simulated data and the experimental data are used to verify the effectiveness of the algorithm in compound fault diagnosis, the results show that the proposed algorithm can successfully extract the expected fault signals with a stable convergence behavior.

REFERENCES

[1] R. Yuan, Y. Lv, H. Li, and G. Song, "Robust fault diagnosis of rolling bearings using multivariate intrinsic multiscale entropy analysis and neural network under varying operating conditions," *IEEE Access*, vol. 7, pp. 130804–130819, 2019.
[2] Z. Chen, J. Cen, and J. Xiong, "Rolling bearing fault diagnosis using time-frequency analysis and deep transfer convolutional neural network," *IEEE Access*, vol. 8, pp. 150248–150261, 2020.
[3] M. Ge, Y. Lv, and Y. Ma, "Research on multichannel signals fault diagnosis for bearing via generalized non-convex tensor robust principal component analysis and tensor singular value kurtosis," *IEEE Access*, vol. 8, pp. 178425–178449, 2020.
[4] G. Wang, Z. He, X. Chen, and Y. Lai, "Basic research on machinery fault diagnosis what is the prescription," *J. Mech. Eng.*, vol. 49, no. 1, pp. 63–72, 2013.
[5] Z. Zhan, Q. Liu, T. Fang, Y. Liu, and S. Wang, "Data-driven multimodal operation monitoring and fault diagnosis of high-speed train bearings," *SCIENTIA SINICA Informationis*, vol. 50, no. 4, pp. 527–539, Apr. 2020.
[6] H. Ai jun and Z. Jun, "Diagnosis of multiple faults in rolling bearings based on adaptive maximum correlated kurtosis deconvolution," *J. Vib., Shock*, vol. 38, no. 22, pp. 171–177 and 136, 2019.
[7] W. P. Liu, Y. Q. Liu, and S. P. Yang, "Fault diagnosis of rolling bearing based on typical correlated Kurtogram," *J. Vibrat. Shock*, vol. 37, no. 8, pp. 89–93, 2018.
[8] X. Y. Zhong, H. L. Tian, C. H. Zhao, B. Chen, and F. Chen, "Fault feature extraction for rolling bearings weak faults based on iterative filtering and fast Kurtogram," *J. Vibrat. Shock*, vol. 37, no. 9, pp. 190–195, 2018.
[9] Y. Wang and M. Liang, "Identification of multiple transient faults based on the adaptive spectral kurtosis method," *J. Sound Vib.*, vol. 331, no. 2, pp. 470–486, 2012.
[10] Y. Hu, W. Bao, X. Tu, F. Li, and K. Li, "An adaptive spectral kurtosis method and its application to fault detection of rolling element bearings," *IEEE Trans. Instrum. Meas.*, vol. 69, no. 3, pp. 739–750, Mar. 2020.
[11] J. Gu and Y. Peng, "An improved complementary ensemble empirical mode decomposition method and its application in rolling bearing fault diagnosis," *Digit. Signal Process.*, vol. 113, Jun. 2021, Art. no. 103050.
[12] G. Yu, "A concentrated time–frequency analysis tool for bearing fault diagnosis," *IEEE Trans. Instrum. Meas.*, vol. 69, no. 2, pp. 371–381, Feb. 2020.
[13] C. Wang, "A sample entropy inspired affinity propagation method for bearing fault signal classification," *Digit. Signal Process.*, vol. 102, Jul. 2020, Art. no. 102740.
[14] K. Zhang, X. Chen, L. Liao, M. Tang, and J. Wu, "A new rotating machinery fault diagnosis method based on local oscillatory-characteristic decomposition," *Digit. Signal Process.*, vol. 78, pp. 98–107, Jul. 2018.
[15] D. Zhu, Q. Gao, D. Sun, Y. Lu, and S. Peng, "A detection method for bearing faults using null space pursuit and S transform," *Signal Process.*, vol. 96, pp. 80–89, Mar. 2014.
[16] Z. Guo, M. Liu, Y. Wang, and H. Qin, "A new fault diagnosis classifier for rolling bearing united multi-scale permutation entropy optimize VMD and cuckoo search SVM," *IEEE Access*, vol. 8, pp. 153610–153629, 2020.
[17] T. Han, L. Zhang, Z. Yin, and A. C. C. Tan, "Rolling bearing fault diagnosis with combined convolutional neural networks and support vector machine," *Measurement*, vol. 177, Jun. 2021, Art. no. 109022.
[18] S. S. Udmale and S. K. Singh, "Application of spectral kurtosis and improved extreme learning machine for bearing fault classification," *IEEE Trans. Instrum. Meas.*, vol. 68, no. 11, pp. 4222–4233, Nov. 2019.
[19] Y. Zhang, Z. Ren, and S. Zhou, "An intelligent fault diagnosis for rolling bearing based on adversarial semi-supervised method," *IEEE Access*, vol. 8, pp. 149868–149877, 2020.
[20] X. Y. Hu, Y. J. Jing, Z. K. Song, and Y. Q. Hou, "Bearing fault identification by using deep convolution neural networks based on CNN-SVM," *J. Vibrat. Shock*, vol. 38, no. 18, pp. 173–178, 2019.
[21] T. Lu, F. Yu, B. Han, and J. Wang, "A generic intelligent bearing fault diagnosis system using convolutional neural networks with transfer learning," *IEEE Access*, vol. 8, pp. 164807–164814, 2020.
[22] Z. Zheng, J. Fu, C. Lu, and Y. Zhu, "Research on rolling bearing fault diagnosis of small dataset based on a new optimal transfer learning network," *Measurement*, vol. 177, Jun. 2021, Art. no. 109285.
[23] F. Xue, W. Zhang, F. Xue, D. Li, S. Xie, and J. Fleischer, "A novel intelligent fault diagnosis method of rolling bearing based on two-stream feature fusion convolutional neural network," *Measurement*, vol. 176, May 2021, Art. no. 109226.
[24] W. Mao, J. Chen, X. Liang, and X. Zhang, "A new online detection approach for rolling bearing incipient fault via self-adaptive deep feature matching," *IEEE Trans. Instrum. Meas.*, vol. 69, no. 2, pp. 443–456, Feb. 2020.
[25] X. Li, W. Zhang, and Q. Ding, "Understanding and improving deep learning-based rolling bearing fault diagnosis with attention mechanism," *Signal Process.*, vol. 161, pp. 136–154, Aug. 2019.
[26] Y. J. Jia and P. F. Xu, "Blind separation of mixed audio signal based on FastICA," *J. THz Sci. Electron. Inf. Technol.*, vol. 7, no. 4, pp. 321–325, 2009.
[27] R. Yang, Y. Jin, L. Hou, and Y. Chen, "Super-harmonic resonance characteristic of a rigid-rotor ball bearing system caused by a single local defect in outer raceway," *Scientia Sinica Technologica*, vol. 49, pp. 117–118, Aug. 2019.
[28] H. H. Dam, D. Rimantho, and S. Nordholm, "Second-order blind signal separation with optimal step size," *Speech Commun.*, vol. 55, no. 4, pp. 535–543, May 2013.
[29] W. T. Zhang, S. T. Lou, and D. Z. Feng, "Adaptive quasi-Newton algorithm for source extraction via CCA approach," *IEEE Trans. Neural Netw. Learn. Syst.*, vol. 25, no. 4, pp. 67–89, Apr. 2014.

[30] G. K. Boray and M. D. Srinath, "Conjugate gradient techniques for adaptive filtering," *IEEE Trans. Circuits Syst. I, Fundam. Theory Appl.*, vol. 39, no. 1, pp. 1–10, Jan. 1992.
[31] Y. Notay, "Flexible conjugate gradients," *SIAM J. Sci. Comput.*, vol. 22, no. 4, pp. 1444–1460, Jan. 2000.
[32] (2016). *Case Western Reserve University, Bearing Data Center, Seeded Fault Test Data*. [Online]. Available: http://csegroups.case.edu/bearingdatacenter/home

WEI-TAO ZHANG was born in 1983. He is currently an Associate Professor with the School of Electronic Engineering, Xidian University, China. His research interests include blind signal processing, tensor analysis, and machine learning.

XIAO-FAN JI was born in 1997. She is currently pursuing the Ph.D. degree with the School of Electronic Engineering, Xidian University, China. Her research interests include blind signal processing and fault diagnosis of complex systems.

JU HUANG was born in 1984. He is currently a Senior Engineer at the Research Institute of Guiyang Engine Design of Aero Engine Corporation of China. His research interest includes aero-engine parts design and testing.

SHUN-TIAN LOU (Member, IEEE) was born in 1962. He is currently a Professor with the School of Electronic Engineering, Xidian University, China. His research interests include signal processing, pattern recognition, and intelligent control using neural network and fuzzy systems.